Iranian Journal of Catalysis 7(4), 2017, 249-255

IRANIAN JOURNAL OF CATALYSIS

Activity of Cu-Co-M (M= Ce, Ni, Au, Mg) catalysts prepared by coprecipitation method, calcined at high temperature for CO oxidation

Gaurav Rattan[a], Chirag Khullar[a,*], Maninder Kumar[b]

[a]*Dr. S. S. Bhatnagar University Institute of Chemical Engineering & Technology, Panjab University, Chandigarh, India.*

[b]*Department of Chemical Engineering, Chandigarh University, Mohali, Punjab, India.*

Received 11 January 2017; received in revised form 23 August 2017; accepted 25 August 2017

ABSTRACT

The present study deals with analysis of the activity of catalysts prepared by addition of different metals to Copper and Cobalt based catalysts for CO oxidation and the variation in activity caused by changes in composition. A series of catalysts were prepared with Cu:Co molar ratio 1:4 and a third metal (M= Ce, Ni, Au, Mg) was added in three different quantities. Compositions were prepared by coprecipitation method, calcinated at 550°C for three hours. The results reported that the cerium based catalysts showed the highest activity $T_{100\%}$ = 390°C in terms of CO oxidation whereas gold based catalysts showed the least activity $T_{58.24\%}$ = 418°C. The best selected catalyst of each group was characterized by the Scanning Electron Microscopy (SEM), X-Ray Diffraction (XRD) and Fourier Transform Infrared Spectroscopy (FTIR).

Keywords*: CO Oxidation; Catalyst; Cu-Co; Cerium; Gold; Nickel; Magnesium.*

1. Introduction

Carbon monoxide results from incomplete combustion of fuel and is emitted directly from vehicle tailpipes. Two-thirds of the carbon monoxide emissions come from transportation sources, with the largest contribution coming from highway motor vehicles. In urban areas, the motor vehicle contribution to carbon monoxide pollution can exceed 90 percent [1]. Thus, stringent and continuously changing environmental regulations are being imposed which are to be met by the companies and industries [2–5].

Use of precious metal catalysts for the low temperature oxidation of CO has been predominant [6–12]. However, the high cost and limited availability of the precious metal catalysts have necessitated the development of base metal catalysts for this application [13]. To use low cost catalysts, transition base metal catalysts [14–16] have been studied from the past century and various combinations and techniques for the catalysts have been developed which are as effective as precious metal catalysts. Two of the biggest advantages of base metal catalysts are their low cost and easy availability.

*Corresponding author email: chirag13121@gmail.com
Tel.: +91 98 7212 5806

Copper and Cobalt based catalysts, the two transition base metals [17–19] along with a third metal such as cerium, nickel, magnesium and gold (Ce, Ni, Mg, Au) have been studied thoroughly for CO oxidation.

In this study, catalysts were prepared by coprecipitation method, Copper and Cobalt based catalysts with the molar ratio of Cu:Co in 1:4, and a third metal in different quantities was added. The third metal is cerium, nickel, magnesium and gold (Ce, Ni, Mg, Au). The prepared catalysts were tested for carbon monoxide oxidation. The best selected catalysts of each group were characterized by SEM, XRD and FTIR.

2. Experimental

2.1. Preparation of the catalysts

Copper and Cobalt based catalysts were prepared by the coprecipitation method [17] with addition of a third metal (Ce, Ni, Mg, Au), using nitrate salts or pure elements. Molar ratio of Cu:Co was kept constant at 1:4 and third element varied in quantity. The all chemicals used were of AR grade. The solution of metal nitrates was slowly added to the solution of sodium carbonate in distilled water (0.2 M) under continuous stirring, maintaining pH 10. After a while, precipitates formed were filtered and washed several times with distilled

water and dried in an oven overnight at 100°C. After drying, the samples were calcined in the muffle furnace at 550°C for three hours. The compositions are shown in Table 1. The prepared catalysts were stored in air tight bottles.

2.2. Catalytic activity measurements

The catalytic activity was measured in the tubular packed bed reactor at atmospheric pressure. 100 mg of the catalyst was diluted with 5 gm alumina powder [20] and placed in the reactor. The reactant gas mixture consisted of CO (1 ml/min) [21] and air (99 ml/min), maintaining a total flow rate of 100 ml/min. The flow rate of CO and of air was monitored by digital flow meters (SMART INSTRUMENTS INDIA). The air feed was made free of moisture and carbon dioxide by passing it through CaO and KOH pellets. The catalytic experiments were carried out under steady state conditions. The reactants and products were analyzed using gas chromatograph (NUCON 5765). Conversion of CO was monitored as the temperature of the reactor rises gradually. A K-type controller (NUTRNICS DTC-201) was used to maintain the temperature inside the reactor. Schematic diagram of experiment is shown in Fig. 1. Catalytic activity was expressed in terms of CO conversion, calculated by equation (1).

$$X_{CO} = \frac{(C_{CO,in} - C_{CO,out})}{C_{CO,in}} \quad (1)$$

3. Results and Discussion

3.1. Catalytic activity of the catalysts prepared

The compositions of the catalysts having the variable metals cerium, magnesium, nickel and gold with copper and cobalt in constant molar ratio 1:4 is shown in Table 1. The catalytic activity of the catalysts is expressed in terms of CO conversion at different temperatures as shown in Figs. 2, 3, 4, 5. Various compositions give the CO conversion at different temperatures.

Table 1. Table showing the composition of different catalysts prepared.

Catalyst	Composition (Molar Ratio)	Catalyst ID
Cu:Co:Ce	1:4:0.5	Cat1
	1:4:1	Cat2
	1:4:2	Cat3
Cu:Co:Ni	1:4:0.5	Cat4
	1:4:1	Cat5
	1:4:2	Cat6
Cu:Co:Mg	1:4:0.5	Cat7
	1:4:1	Cat8
	1:4:2	Cat9
Cu:Co:Au	1:4:0.003	Cat10
	1:4:0.0076	Cat11
	1:4:0.0153	Cat12

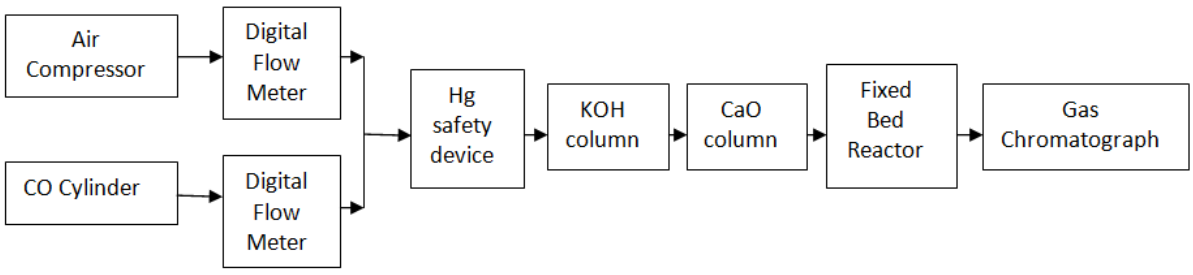

Fig. 1. Schematic diagram of the experiment.

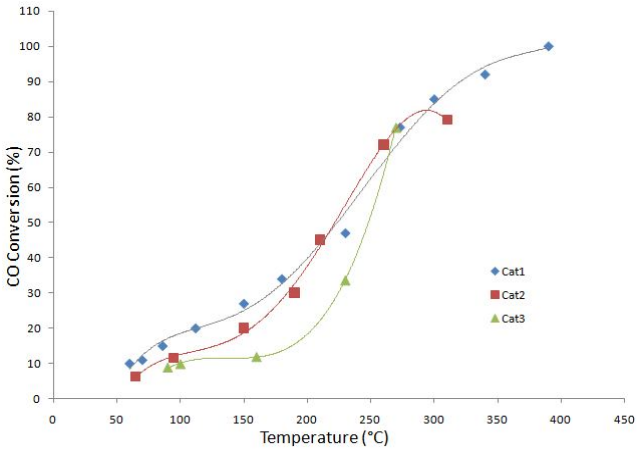

Fig. 2. Catalytic activity of Cu, Co, Ce catalysts at different Cu:Co:Ce ratios (Conditions: Atmospheric pressure, 50°C to temperature with maximum conversion).

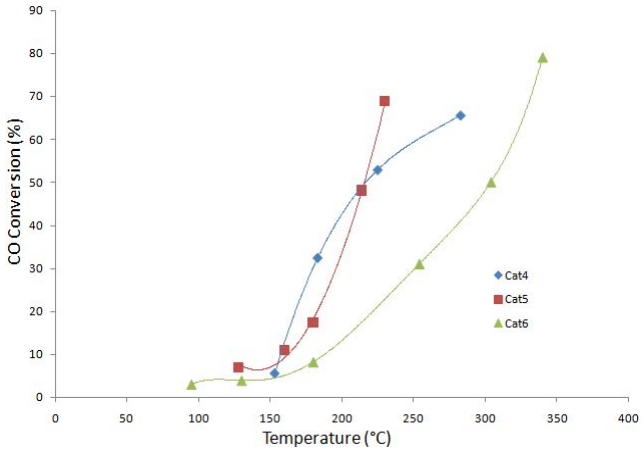

Fig. 3. Catalytic activity of Cu, Co, Ni catalysts at different Cu:Co:Ni ratios (Conditions: Atmospheric pressure, 100°C to temperature with maximum conversion).

It is clearly shown in the graphs that the catalytic activity increased in nickel and magnesium based catalysts as their content in the catalysts was increased and copper and cobalt contents were kept constant. Decrease in catalytic activity of cerium and gold based catalysts were associated with increasing their contents and keeping copper and cobalt contents constant. Of the four groups of catalysts, cerium catalysts showed the highest activity and gold catalysts showed the least activity.

3.2. Characterization

3.2.1. SEM

Morphology of prepared catalysts has been determined by SEM instruments Digital Scanning Electron Microscope - JSM 6100 (JEOL). It has a large specimen chamber that allows observation of the entire surface of a specimen upto 150 mm and a tilt of -5 to 90°.

The catalyst powder is placed directly on double sided sticky carbon tape for analysis. SEM images in Fig. 6 can reveal the formation of thread like structures in nickel based catalyst. The nickel catalyst had long threads and in bulky mass it had globular shaped structures. Even magnesium based catalysts had some thread structures and globular shape but not as lengthy and not as much as in nickel based catalysts. The structures found in nickel catalysts might increase surface area due to which nickel catalyst activity is more than that of magnesium catalyst in which density of similar structures was less. The cerium and gold catalysts had an irregular morphology, the particles had irregular shape without any thread structures like those in nickel and magnesium. The presence of aggregation in the samples may be due to the occurrence of large surface energy and surface tension in the samples due to high temperature treatment [22].

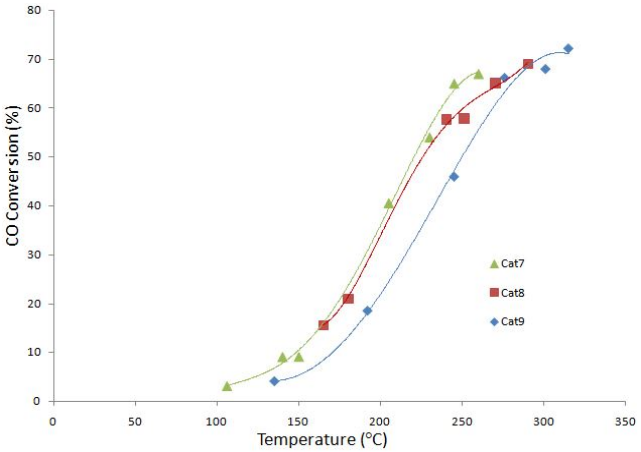

Fig. 4. Catalytic activity of Cu, Co, Mg catalysts at different Cu:Co:Mg ratios (Conditions: Atmospheric pressure, 100°C to temperature with maximum conversion).

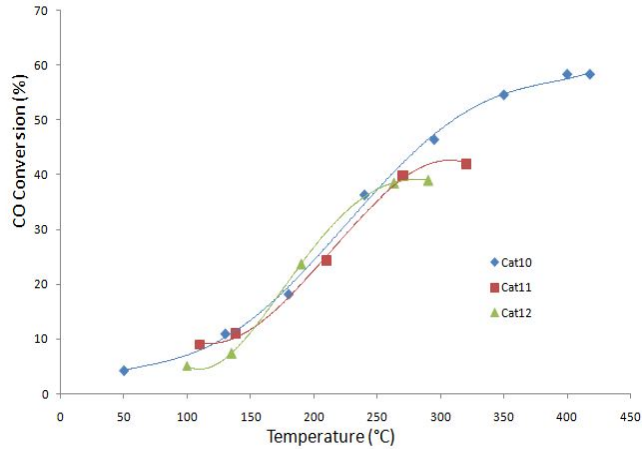

Fig. 5. Catalytic activity of Cu, Co, Au catalysts at different Cu:Co:Au ratios (Conditions: Atmospheric pressure, 50°C to temperature with maximum conversion).

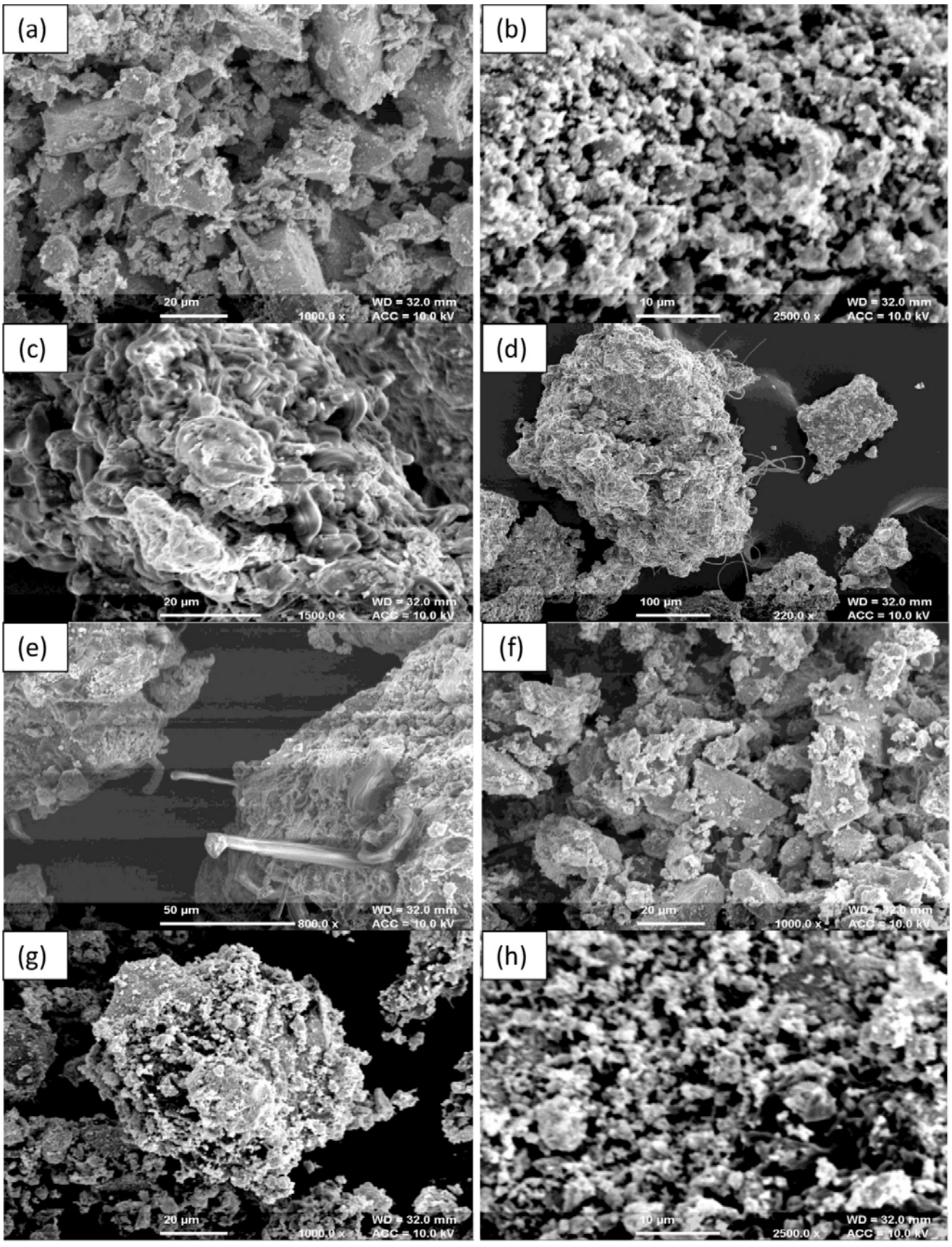

Fig. 6. SEM micrographs of the catalysts (a, b)-Cat1, (c, d)-Cat6, (e, f)-Cat9, (g, h)-Cat10.

The gold catalyst is agglomerated, particle size is large compared to cerium and magnesium catalysts which had a smaller particle size, so gold particles have less surface area for reaction. This is the reason why gold is not as active as others. Cerium catalyst has advantage of both small particle size and high pore density making it highly active catalyst.

3.2.2. X-Ray diffraction

X-Ray diffraction (XRD) of the catalyst samples was carried out to identify the phases and oxidation states present in the catalysts. The Rigaku Ultima IV fully automatic high-resolution X-ray diffractometer system with Theta-Theta (θ-θ) Goniometer for routine characterization of powder samples was used. Standard X-ray Tube with Electro Magnetic shutter, Cu target and long fine focus having operating current and operating voltage of 40 mA and 45 KV respectively was used. The scanning range 2Θ was 5.00 – 110.00° with divergence slit of 2/3°. The continuous scanning was done with the step size of 0.0200. The XRD pattern of the catalysts is shown in the Fig. 7.

The strong peaks are due to cobalt species [23] [JCPDS No. 76-1802], copper species [JCPDS No. 05-0661], cerium species [JCPDS No. 75-0076], 43.39 is due to nickel oxide [JCPDS No. 89-1397], 38.9 is due to gold [JCPDS No.04-0784].

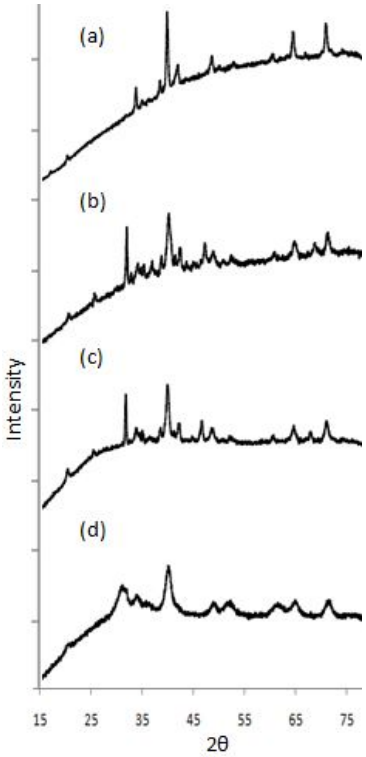

Fig. 7. XRD of catalysts (a)-Cat1, (b)-Cat6, (c)-Cat9, (d)-Cat10.

The diffraction peaks of catalysts showed that the gold, cerium and magnesium catalysts were highly amorphous whereas nickel had crystallinity. The broad diffraction peaks in the catalysts are due to the formation of small crystallites.

At high calcination temperatures, relative intensity of diffraction peaks decreased which might be due to the increase in the lattice disorder and strain induced, since increasing calcination temperature gives atoms more energy to move [24]. In addition, the crystallization in structures increases, which is evident from the number of peaks, formed. The size of crystal grows as the calcinations temperature is increased. At high calcination temperatures, continuous grain boundaries are formed due to bridging of fine particles to increase the crystal size. This causes a reduction in porosity of the catalyst, resulting in a reduction in activity [25].

3.2.3. FTIR

From the FTIR data of Fig. 8, it is observed that the bands are broad which means amorphous phases have been obtained. Clearly well determined bands with well expressed peaks, typical of crystalline substances, can also been observed. XRD proved that catalysts containing nickel exhibit crystalline characteristics [26]. Generally, the characteristic bands shift toward a higher wave number region may be due to the increase in particle size and also there is a significant shift from cerium to gold catalyst which shows that the gold catalyst has particles larger than the other catalysts [25].

Distinctive bands originate from the stretching vibrations of the metal-oxygen bond. As can be seen in Fig. 8, the first band $\bar{\nu}_1$ at around 570 cm^{-1} is associated with the BOB_3 vibrations in the spinel lattice, where B denotes the Co cations in an octahedral position, due to the presence of randomly oriented octahedral, i.e. cobalt is situated in oxygen octahedral environment, i.e. Co^{3+} ions. The second bands $\bar{\nu}_2$ at around 651 cm^{-1} is attributed to the ABO_3 vibrations, where A denotes the metal ions in a tetrahedral position. The spectrum showing bands at 570 and 667 cm^{-1} was assigned to Co_3O_4 [23]. The presence of two absorption bands around 570 and 667 cm^{-1} was assigned to Co-O stretching vibration mode and bridging vibration of O-Co-O bond which originate from the stretching vibrations of the metal-oxygen bond and confirmed the formation of Co_3O_4 spinel oxide [27]. The bands in the range of 1400-850 cm^{-1} are due to stretching of asymmetrical and symmetrical vibrations of B-O bonds in BO_3 and BO_4 groups [26]. Generally, the metal oxides may show absorption bands below 1000 cm^{-1} arising from inter atomic vibrations, stretching and vibrational modes of metal oxygen [28-31].

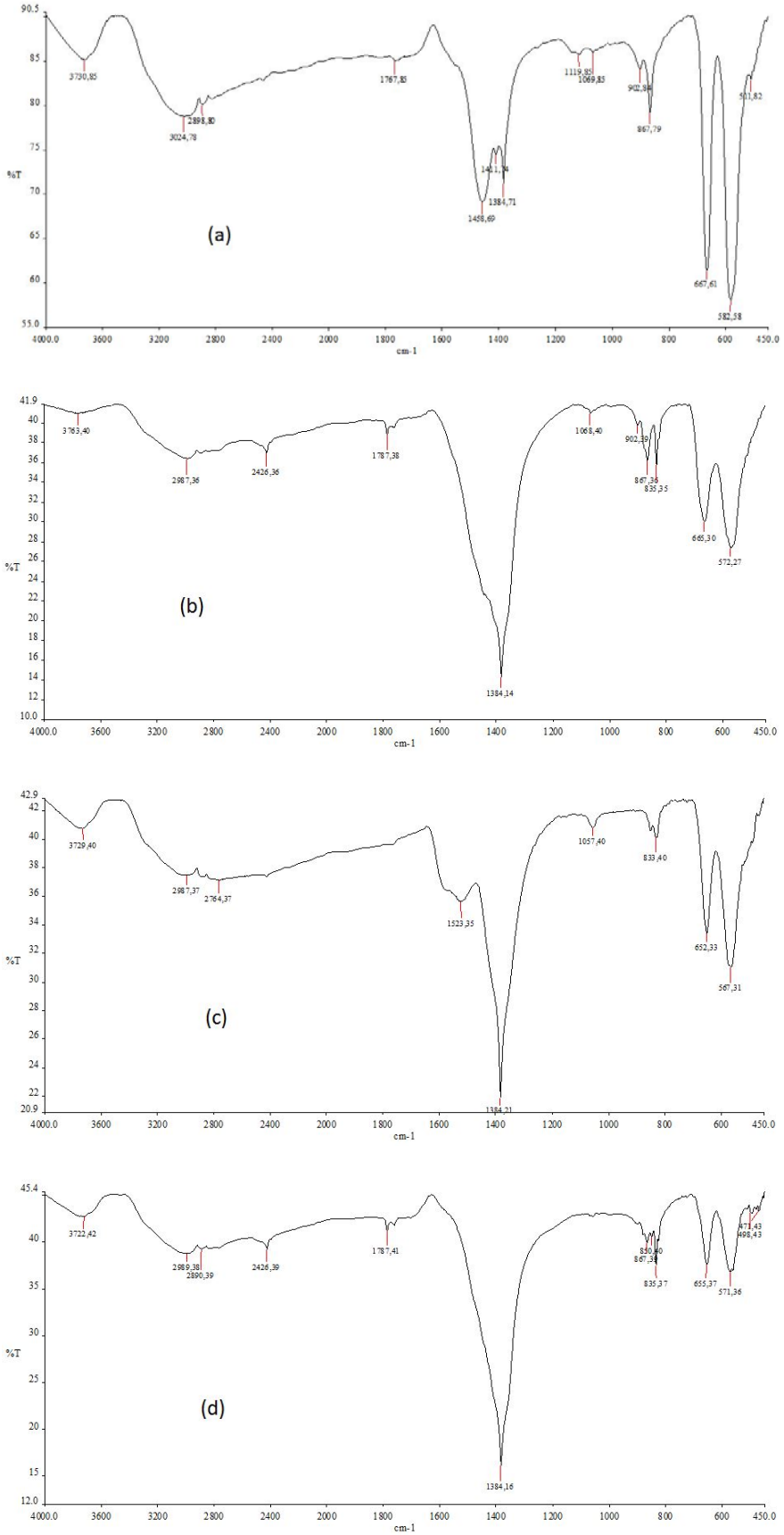

Fig. 8. FTIR of the catalysts (a)-Cat1, (b)-Cat6, (c)-Cat9, (d)-Cat10.

4. Conclusions

Twelve catalysts were prepared by the coprecipitation technique, these catalysts were calcined at 550°C. All the catalysts were tested for CO oxidation.

It has been observed that addition of nickel, magnesium to copper and cobalt catalyst increases its catalytic activity ($T_{65.6\%}$ = 283°C to $T_{79\%}$ = 340°C for nickel, $T_{73.1\%}$ = 340°C to $T_{79.21\%}$ = 391°C for magnesium). However, with addition of cerium and gold, the catalytic activity of copper and cobalt catalyst decreased ($T_{100\%}$ = 390°C to $T_{77\%}$ = 270°C for cerium, $T_{58.24\%}$ = 418°C to $T_{39\%}$ = 290°C for gold). Catalysts having cerium showed the best activity in comparison to others, whereas gold catalysts showed the least activity.

The SEM analysis showed that nickel catalyst had a globular structure with thread-like projections, this might enhance activity with increasing nickel content. As the globular structures increase, the surface area might also increase. Agglomeration of the gold catalyst might result in its lower activity.

XRD and FTIR analyses showed that nickel had a high crystallinity in comparison to cerium, magnesium and gold catalysts. The particle size of gold catalysts was also larger than other catalysts.

Acknowledgements

Technical Education Quality Improvement Programme (TEQIP-II) has provided the financial support for this research. The authors thank X-ray Facility at IISER Mohali for helping in XRD analysis, SAIF Facility at Panjab University for SEM, FTIR analysis.

References

[1] H. Kebin, Z. Qiang, H. Hong, Point Sources of Pollution: Local Effects and their Control, EOLLS Publishers, Oxford, 2009.
[2] W. Liu, M.F. Stephanopoulos, J. Catal. 153 (1995) 304-316.
[3] S.H. Taylor, G.J. Hutchings, A.A. Mirzaei, Chem. Commun. (1999) 1373-1374.
[4] D.M. Whittle, A.A. Mirzaei, J.S.J. Hargreaves, R.W. Joyner, C.J. Kiely, S.H. Taylor, G.J. Hutchings, Phys. Chem. Chem. Phys. 4 (2002) 5915-5920.
[5] Y. Choi, H.G. Stenger, J. Power Sources 129 (2004) 246-254.
[6] R.M.T. Sanchez, A. Ueda, K. Tanaka, M. Haruta, J. Catal. 168 (1997) 125-127.
[7] M. Haruta, S. Tsubota, T. Kobayashi, H. Kageyama, M.J. Genet, B. Delmon, J. Catal. 144 (1993) 175-192.
[8] A. Wolf, F. Schuth, Appl. Catal. A 226 (2002) 1-13.
[9] F. Moreau, G.C. Bond, A.O. Taylor, Chem. Commun. (2004) 1642-1643.
[10] B. Qiao, Y. Deng, Chem. Commun. (2003) 2192-2193.
[11] W. Yan, B. Chen, S.M. Mahurin, S. Dai, S.H. Overbury, Chem. Commun. (2004) 1918-1919.
[12] M. Koudiakov, M.C. Gupta, S. Deevi, Nanotechnology 15 (2004) 987-990.
[13] M. Kang, M.W. Song, C.H. Lee, Appl. Catal. A 251 (2003) 143-156.
[14] S.M. Eyubova, V.D. Yagodovskii, Russ. J. Phys. Chem. A 81 (2007) 544-548.
[15] M. Mokhtar, S.N. Basahel, Y.O. Al-Angary, J. Alloys Compd. 493 (2010) 376-384.
[16] Z. Zhao, M.M. Yung, U.S. Ozkan, Catal. Commun. 9 (2008) 1465-1471.
[17] M. Kang, M.W. Song, C.H. Lee, Appl. Catal. A 251 (2003) 143-156.
[18] C.B. Wang, C.W. Tang, W.C. Tsai, M.C. Kuo, S.H. Chien, Catal. Lett. 107 (2006) 31-37.
[19] G. Rattan, M. Kumar, Chem. Chem. Technol. 8 (2014) 249-260.
[20] G. Rattan, R. Prasad, R.C. Katyal, Bull. Chem. React. Eng. Catal. 7 (2012) 112-123.
[21] L.P. Ma, H.J. Bart, P. Ning, A. Zhang, G. Wu, Z. Zengzang, Chem. Eng. J. 155 (2009) 241-247.
[22] A. Gulino, P. Dapporto, P. Rossi, I. Fragala, Chem. Mater. 15 (2003) 3748-3752.
[23] C.W. Tang, T.Y. Leu, W.Y. Yu, C.B. Wang, S.H. Chien, Thermochim. Acta 473 (2008) 68-73.
[24] M. Bordbar, S.M. Vasegh, S. Jafari, A.Y. Faal, Iran. J. Catal. 5 (2015) 135-141.
[25] K.K. Babitha, A. Sreedevi, K.P. Priyanka, B. Sabu, T. Varghese, Indian J. Pure Appl. Phys. 53 (2015) 596-603.
[26] M. Deneva, J. Univ. Chem. Technol. Metall. 45 (2010) 351-378.
[27] M.M.J. Sadiq, A.S. Nesaraj, Iran. J. Catal. 4 (2014) 219-226.
[28] B. Khodadadi, M. Bordbar, Iran. J. Catal. 6 (2016) 37-42.
[29] A. Pourtaheri, A. Nezamzadeh-Ejhieh, Chem. Eng. Res. Design 104 (2015) 835-843.
[30] H. Derikvandi, A. Nezamzadeh-Ejhieh, J. Hazard Mater. 321 (2017) 629-638.
[31] A. Shirzadi, A. Nezamzadeh-Ejhieh, J. Mol. Catal. A: Chem. 411 (2016) 222-229.